Strain effects on optical polarisation properties in (11$\bar{2}$2) plane GaN films*

Hao Guo-Dong(郝国栋)[a)†], Chen Yong-Hai(陈涌海)[b)], Fan Ya-Ming(范亚明)[a)], Huang Xiao-Hui(黄晓辉)[a)], and Wang Huai-Bing(王怀兵)[a)]

[a)] *Nano-Devices and Materials Division, Suzhou Institute of Nano-tech and Nano-bionics, Chinese Academy of Sciences, Suzhou* 215125, *China*

[b)] *Key Laboratory of Semiconductor Materials Science, Institute of Semiconductors, Chinese Academy of Sciences, Beijing* 100083, *China*

(Received 25 December 2009; revised manuscript received 21 June 2010)

We present the theoretical results of the electronic band structure of wurtzite GaN films under biaxial strains in the (11$\bar{2}$2)-plane. The calculations are performed by the $\boldsymbol{k}\cdot\boldsymbol{p}$ perturbation theory approach through using the effective-mass Hamiltonian for an arbitrary direction. The results show that the transition energies decrease with the biaxial strains changing from -0.5% to 0.5%. For films of (11$\bar{2}$2)-plane, the strains are expected to be anisotropic in the growth plane. Such anisotropic strains give rise to valence band mixing which results in dramatic change in optical polarisation property. The strain can also result in optical polarisation switching phenomena. Finally, we discuss the applications of these properties to the (11$\bar{2}$2) plane GaN-based light-emitting diode and lase diode.

Keywords: GaN, (11-22)-plane, strain, optical anisotropy

PACC: 7115T, 7865K, 4225J

1. Introduction

III–V wurtzite nitrides such as GaN or InGaN have been under extensive examination for many years because of their promising applications in short-wavelength light emitting devices.[1−3] Most of the efforts have been made to study the structures grown along the [0001] direction.[4] In these structures, internal electric fields are induced in the strained layers, which separate the electrons from the holes, thereby reducing the radiative efficiency and overall device performance. In addition, recent researches show that the polarisation field is one of the physical origins of the efficiency droop for devices operating at high powers.[5,6] One way to circumvent these problems is to grow quantum wells (QWs) on nonpolar or semipolar planes where these electric fields are theoretically diminished or even eliminated.[7] Another advantage for GaN devices grown on nonpolar or semipolar plane is that they exhibit optical gain anisotropy which leads to polarised light emission.[8,9] Although the high power M-plane light-emitting diode (LED) has been demonstrated,[10] the semipolar (11$\bar{2}$2) plane might have an advantage of incorporating higher In content relative to the nonpolar M-plane and A-plane, as evidenced by the demonstration of a yellow LED[11] and green light emitters.[12] The semipolar (11$\bar{2}$2) plane violet lase diodes (LDs) with continuous-wave operations have also been demonstrated.[13] It has also been proposed to be unique among low-index semipolar orientation.[14]

A knowledge of the polarisation characteristics is of importance not only for solid-state physics, but also for practical application to device fabrication. Taking LD as an example, the resonant cavities can be constructed with cleaved facet mirrors for the principal polarisation parallel to the (1$\bar{1}$00) plane, whereas it is unlikely to find a low-index plane perpendicular to (1$\bar{1}$23) if the principal polarisation happens to be parallel to (1$\bar{1}$00). The optical properties depend on crystal-orientation and quantum well width, which has been discussed in Refs. [15]–[17]. The polarisation ratio increases with the increase of indium composition for the semi-polar (11$\bar{2}$2) plane, which has been investigated in Ref. [18]. The optical gain of the (11$\bar{2}$2)-oriented QW is significantly larger than that of the (0001)-oriented QW.[19] The opti-

*Project supported by the National Basic Research Program of China (Grant Nos. 2006CB604908 and 2006CB921607), and the National Natural Science Foundation of China (Grant Nos. 60625402, 60990313 and 60990311).

†Corresponding author. E-mail: gdhao@semi.ac.cn

© 2010 Chinese Physical Society and IOP Publishing Ltd

cal polarisation switching phenomena were also observed in $\{11\bar{2}2\}$ GaN QWs with various well widths and In compositions.[20,21] The electronic band structure (EBS) and the polarisation characteristics of group-III-nitride are sensitive to strains. These aspects have been extensively studied for the polar (C-) plane and non-polar (A- and M-) planes of wurtzite-GaN.[4,22−26] However, there has been very little work on strain effects on electronic and optical properties of GaN epitaxial layer with the $(11\bar{2}2)$ crystal orientation, and further investigation is needed. This is the main motivation of this work.

In this paper, according to the Hamiltonian of a strained wurtzite semiconductor with an arbitrary orientation presented in our previous study,[27] we theoretically investigate the strain dependence on the EBS of $(11\bar{2}2)$ plane GaN . We also study the strain effects on the optical polarisation properties of the three transitions. Finally, we discuss the implications of these properties for device application based on $(11\bar{2}2)$ plane GaN.

2. Theory

The Cartesian coordinate system (X, Y, Z) can be attached to the primary crystallographic axes. Z' is in an arbitrary direction perpendicular to the growth plane, Y' is along $[1\bar{1}00]$ direction, X' is perpendicular to Y' and Z', in the set of basis functions:

$$\begin{aligned}
|1\rangle &= \alpha^* \left| -\frac{(X'+\mathrm{i}Y')}{\sqrt{2}} \uparrow' \right\rangle - \alpha \left| \frac{(X'-\mathrm{i}Y')}{\sqrt{2}} \downarrow' \right\rangle, \\
|2\rangle &= \beta \left| \frac{(X'-\mathrm{i}Y')}{\sqrt{2}} \uparrow' \right\rangle - \beta^* \left| -\frac{(X'+\mathrm{i}Y')}{\sqrt{2}} \downarrow' \right\rangle, \\
|3\rangle &= -\beta^* |Z' \uparrow'\rangle + \beta |Z' \downarrow'\rangle, \\
|4\rangle &= \alpha^* \left| -\frac{(X'+\mathrm{i}Y')}{\sqrt{2}} \uparrow' \right\rangle + \alpha \left| \frac{(X'-\mathrm{i}Y')}{\sqrt{2}} \downarrow' \right\rangle, \\
|5\rangle &= \beta \left| \frac{(X'-\mathrm{i}Y')}{\sqrt{2}} \uparrow' \right\rangle + \beta^* \left| -\frac{(X'+\mathrm{i}Y')}{\sqrt{2}} \downarrow' \right\rangle, \\
|6\rangle &= \beta^* |Z' \uparrow'\rangle + \beta |Z' \downarrow'\rangle, \qquad (1)
\end{aligned}$$

where $\alpha = \exp(\mathrm{i}3\pi/4)/\sqrt{2}$, and $\beta = \exp(\mathrm{i}\pi/4)/\sqrt{2}$. The 6×6 Hamiltonian in the (X', Y', Z') coordinates can be block-diagonalized into two 3×3 matrices.

$$\boldsymbol{H}'_v(\epsilon, k'=0) = \begin{bmatrix} H'^{\mathrm{L}} & 0 \\ 0 & H'^{\mathrm{U}} \end{bmatrix}, \qquad (2)$$

$$\boldsymbol{H}'^{\mathrm{U}} = (H'^{\mathrm{L}})^* = \begin{bmatrix} F' & K' & -\mathrm{i}I' \\ K' & G' & \Delta - \mathrm{i}I' \\ \mathrm{i}I' & \Delta + \mathrm{i}I' & \lambda' \end{bmatrix}, \qquad (3)$$

where

$$\begin{aligned}
F' &= \Delta_1 + \Delta_2 - \frac{\Delta_1 \sin^2\theta}{2} + \xi_\epsilon, \\
G' &= \Delta_1 - \Delta_2 - \frac{\Delta_1 \sin^2\theta}{2} + \xi_\epsilon, \\
\lambda' &= \Delta_1 \sin^2\theta + \lambda_\epsilon, \\
K' &= -\frac{\Delta_1 \sin^2\theta}{2} + K_\epsilon, \\
I' &= \frac{\Delta_1 \sin\theta\cos\theta}{\sqrt{2}} + I_\epsilon, \\
\Delta &= \sqrt{2}\Delta_3, \\
\xi_\epsilon &= D_1\epsilon_{zz} + D_2(\epsilon_{xx}+\epsilon_{yy}) + \frac{1}{2}\{[D_3\epsilon_{zz} + D_4(\epsilon_{xx}+\epsilon_{yy})](1+\cos^2\theta) \\
&\quad -D_5(\epsilon_{xx}-\epsilon_{yy})\sin^2\theta - \sqrt{2}D_6\epsilon_{xz}\sin(2\theta)\}, \\
\lambda_\epsilon &= D_1\epsilon_{zz} + D_2(\epsilon_{xx}+\epsilon_{yy}) + [D_3\epsilon_{zz} + D_4(\epsilon_{xx}+\epsilon_{yy}) + D_5(\epsilon_{xx}-\epsilon_{yy})]\sin^2\theta + \sqrt{2}D_6\epsilon_{xz}\sin(2\theta), \\
K_\epsilon &= \frac{1}{2}\{[D_3\epsilon_{zz} + D_4(\epsilon_{xx}+\epsilon_{yy})](-\sin^2\theta) + D_5(\epsilon_{xx}-\epsilon_{yy})(1+\cos^2\theta) \\
&\quad -\sqrt{2}D_6\epsilon_{xz}\sin(2\theta) - 2\sqrt{2}\mathrm{i}D_6\epsilon_{yz}\sin\theta + 4\mathrm{i}D_5\epsilon_{xy}\cos\theta\}, \\
I_\epsilon &= \frac{1}{\sqrt{2}}\{[D_3\epsilon_{zz} + D_4(\epsilon_{xx}+\epsilon_{yy}) + D_5(\epsilon_{xx}-\epsilon_{yy})]\sin\theta\cos\theta \\
&\quad +\sqrt{2}D_6\epsilon_{xz}\cos(2\theta) + \sqrt{2}\mathrm{i}D_6\epsilon_{yz}\cos\theta + 2\mathrm{i}D_5\sin\theta\epsilon_{xy}\}. \qquad (4)
\end{aligned}$$

The symbol $*$ means taking complex conjugate, and the parameters $D_1, D_2, D_3, D_4, D_5, D_6, \Delta_1, \Delta_2$ and Δ_3 are as they are defined in Ref. [28]. The strain tensor ϵ_{ij} can be substituted by $\epsilon_{k'l'}$ according Ref. [27].

The conduction-band edge has a hydrostatic energy shift $P_{c\epsilon}$, and it satisfies

$$\begin{aligned} E_c &= E_v^0 + \Delta_1 + \Delta_2 + E_{\rm g} + P_{c\epsilon}, \\ P_{c\epsilon} &= a_{cz}\epsilon_{z'z'} + a_{ct}(\epsilon_{x'x'} + \epsilon_{y'y'}). \end{aligned} \tag{5}$$

The transition energies are given by

$$E_j = E_c - E_j^v. \tag{6}$$

The band energy gap $E_{\rm g}$ in GaN is 3.44 eV, a_{cz} and a_{ct} are the conduction-band deformation potentials in the directions along the c axis and perpendicular to the c axis, respectively. We take $a_{cz} = a_{ct}$ for simplicity, and assume a value of –4.6 eV.[29]

The conduction-band wave function of a bulk wurtzite semiconductor can be written as

$$\Psi^{c\eta}(\boldsymbol{k}', \boldsymbol{r}', \boldsymbol{\epsilon}') = \frac{1}{\sqrt{V}} \, {\rm e}^{{\rm i}\boldsymbol{k}'\cdot\boldsymbol{r}'} |S\eta\rangle, \tag{7}$$

where $\eta = \uparrow$ or $\downarrow$, and S is the spherically symmetric wave function. The complete Bloch wave functions for the valence-band are given by

$$\Psi^{v}(\boldsymbol{k}', \boldsymbol{r}', \boldsymbol{\epsilon}') = \frac{1}{\sqrt{V}} \, {\rm e}^{{\rm i}\boldsymbol{k}'\cdot\boldsymbol{r}'} \sum_{i=1}^{6} g_i'(\boldsymbol{k}', \boldsymbol{\epsilon}')|{\rm i}\rangle. \tag{8}$$

The squared magnitudes of the optical matrix element can be expressed as

$$\begin{aligned} |M_{x'}|^2 &= \left| \frac{-(g_1' + g_4')\alpha^* + (g_2' + g_5')\beta}{\sqrt{2}} (P_2 \cos^2\theta + P_1 \sin^2\theta) + (-g_3' + g_6')\beta^* (P_2 - P_1)\cos\theta\sin\theta \right|^2 \\ &\quad + \left| \frac{(-g_1' + g_4')\alpha + (g_2' - g_5')\beta^*}{\sqrt{2}} (P_2 \cos^2\theta + P_1 \sin^2\theta) + (g_3' + g_6')\beta (P_2 - P_1)\cos\theta\sin\theta \right|^2, \end{aligned} \tag{9}$$

$$|M_{y'}|^2 = \left| -\frac{(g_1' + g_4')\alpha^* + (g_2' + g_5')\beta}{\sqrt{2}} P_2 \right|^2 + \left| \frac{(g_1' - g_4')\alpha + (g_2' - g_5')\beta^*}{\sqrt{2}} P_2 \right|^2, \tag{10}$$

$$\begin{aligned} |M_{z'}|^2 &= \left| \frac{-(g_1' + g_4')\alpha^* + (g_2' + g_5')\beta}{\sqrt{2}} (P_2 - P_1)\cos\theta\sin\theta + (-g_3' + g_6')\beta^* (P_1 \cos^2\theta + P_2 \sin^2\theta) \right|^2 \\ &\quad + \left| \frac{(-g_1' + g_4')\alpha + (g_2' - g_5')\beta^*}{\sqrt{2}} (P_2 - P_1)\cos\theta\sin\theta + (g_3' + g_6')\beta (P_1 \cos^2\theta + P_2 \sin^2\theta) \right|^2. \end{aligned} \tag{11}$$

The unit of the matrix element is $P_2 = \langle S|P_x|X\rangle = \langle S|P_y|Y\rangle$, $P_1 = \langle S|P_z|Z\rangle$.

3. Results and discussion

We have calculated the transition energies and the polarisation properties in strained wurtzite GaN. The original data of material parameters are cited from Ref. [29]. We adopt a nomenclature[24] where the top three valance-bands are labeled as $T1, T2$ and $T3$ in the order of increasing transition energies to the conduction-band $E_{T1} < E_{T2} < E_{T3}$, respectively. For $(11\bar{2}2)$ plane, the polar angle $\theta = 58.4°$, the direction of the y' axis lies in the $[1\bar{1}00]$ direction, and the x' axis lies in the $[11\bar{2}\bar{3}]$ direction, z' is perpendicular to the $(11\bar{2}2)$ plane, as shown in Fig. 1. We take the conventional strain to be negative for the compression case, and restrict the in-plane strains in ranges of $|\epsilon_{x'x'}|$ and $|\epsilon_{y'y'}| \leq 0.5\%$.

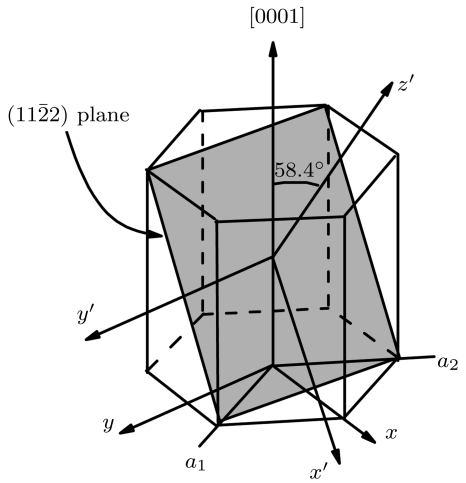


Fig. 1. Configuration of the coordinate systems (x', y', z') in $(11\bar{2}2)$ plane crystals, where the growth axis, or z' axis, is normal to the substrate surface $(11\bar{2}2)$, and the coordinate system (x, y, z) denotes the primary crystallographic axes.

Figures 2(a)–2(c) illustrate the transition energies for the E_{T1}, E_{T2}, E_{T3} in the $(11\bar{2}2)$ plane as functions of the biaxial strains $\epsilon_{x'x'}$ and $\epsilon_{y'y'}$. The transition energies decrease with the strains changing from

−0.5% to 0.5%, which is similar to those in the A- and M-planes.[24−26] Figure 2(d) displays the energy splitting $E_{T2} - E_{T1}$. At the point ($\epsilon_{x'x'} = 0.2\%$, $\epsilon_{y'y'} = 0.38\%$) denoted by the dot lines, the energy difference $E_{T2} - E_{T1}$ is the lowest but neither equal to nor smaller than zero, which means the biaxial strains hardly cause the top two valence-bands to be degenerate or crossed over because of the strong spin-orbit interaction. On the other hand, the energy difference between $T1$ and $T2$ bands increases with the opposite strains (compressive strain along $x'(y')$ direction together with tensile strain along $y'(x')$). For comparison, when a zinc-blende layer is grown along the (001) axis with compressive strain, the strain deformation potentials lift the HH band up and reduce its in-plane effect mass.[30] Thus it is expected that the in-plane effective mass is largely reduced for opposite strains and almost the same as that in the unstrained case for other cases. Unfortunately, there is no experimental result reported which may be compared with our result. Furthermore, in order to reduce the valence band edge density of the state, which is favorable for bringing down the threshold current density of LD, Fig. 2(d) is instructive since we can efficiently separate $T1$ and $T2$ by modulating the strain state of the GaN films.

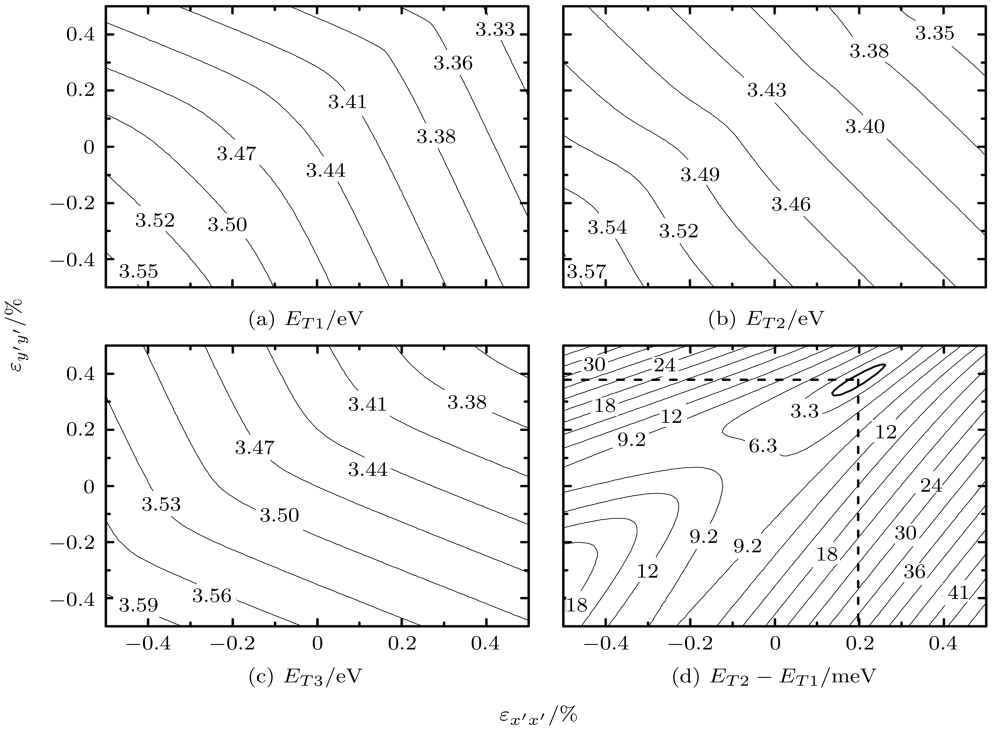


Fig. 2. Calculated transition energies (a) $T1$, (b) $T2$, (c) $T3$, as functions of in-plane strains $\epsilon_{x'x'}$ and $\epsilon_{y'y'}$ for an $(11\bar{2}2)$ plane GaN film and (d) energy difference $T2 - T1$ as functions of in-plane strains $\epsilon_{x'x'}$ and $\epsilon_{y'y'}$.

The strains cause the mixing effects of the three bands which can cause a redistribution of the polarisation properties as shown in Fig. 3 by the gray-scale contour plots. The white area represents pure linear polarisation while the black area denotes forbidden polarisation. Note that the sum rules are also satisfied. For the $T1$ band, which has the lowest transition energy, the transition is dominated by the z'-polarisation in area-3 and x'-polarisation, with a small amount of mixing with z'-polarisation in area-1. Taking the laser cavity in the y' direction as an example, it is helpful to enhance the radiative efficiency in the transverse electric (TE) (transverse magnetic (TM) mode) mode in area-1 (in area-3). For LED, the $T1$ transition is easily extracted out of the film surface in area-1 and area-3 (output light in the y' direction), which can realize high surface emission efficiency (SEE). Meanwhile, pure linear polarisation light emissions can also be obtained, which is favourable for designing polarized photodevices.[9] On the contrary, in area-2, the band is dominated by y'-polarisation, which means that the light emission from the surface plane will be restrained, since light with $E \parallel y'$ does not travel along the y' direction. Then the SEE under these strain conditions is expected to be sufficiently low and thus should be avoided.

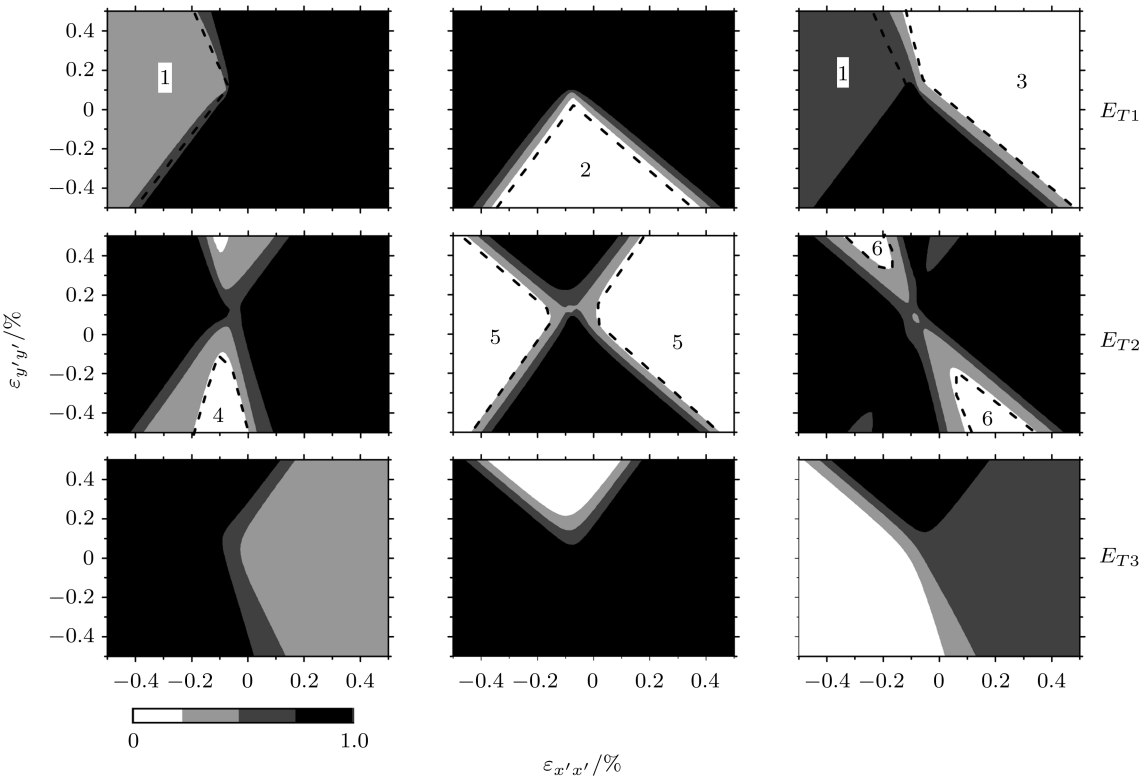


Fig. 3. Relative squared optical matrix elements of x'-, y'- and z'-polarisation lights as functions of in-plane strains $\epsilon_{x'x'}$ and $\epsilon_{y'y'}$ for an $(11\bar{2}2)$ plane GaN.

In contrast to the $T1$ band, the $T2$ band is dominated by x'-, y'- and z'-polarisations in area-4, 5 and 6, respectively. The observations of optical polarisation switching phenomena are revealed in semipolar $\{11\bar{2}2\}$ QWs with various well widths and In compositions.[20,21] A crossover between the top two valance-bands and a large deformation potential of InN were proposed as the mechanism of the polarisation switching. However, our results show that the strains can also result in polarisation switching without the crossover between the top two valance-bands $T1$ and $T2$. The $T3$ band is far from the top of the valence-bands, and has little contribution to the optical transition. Note that the exact values of the deformation potentials $D1$–$D6$ are still under investigation. Hence, the values of the calculated transition energies and optical polarisation may change somewhat, but the overall strain dependence will not be significantly affected.

The above study suggests that, if edge-emitting lasers are realized with $(11\bar{2}2)$-plane GaN in the active region, inducing the strains in area-1 is helpful to enhance the radiative efficiency in the TE mode for output light in y' direction. On the other hand, the strains in area-3 are useful for improving the radiative efficiency in the TM mode. In both area-1 and area-3, the strains are favourable for enhancing the SEE for LED with output light in the y' direction. These are very useful information for realizing the practical GaN-based LD and LED.

4. Conclusion

We have theoretically studied the strain effects on $(11\bar{2}2)$-plane wurtzite GaN crystal. The transition energies and the polarisation properties have been calculated for the $(11\bar{2}2)$-plane on the basis of $\boldsymbol{k}\cdot\boldsymbol{p}$ theory. For the $(11\bar{2}2)$-plane, the transition energies decrease when the strains change from -0.5% to 0.5%. The biaxial strains can significantly change the polarisation properties of three transitions and realize optical polarisation switching phenomena in $(11\bar{2}2)$ plane wurtzite GaN. These analytical expressions and numerical calculations will be useful for understanding the band edge optical properties of GaN and designing optoelectronic devices based on $(11\bar{2}2)$ plane GaN crystal.

References

[1] Nakamura S, Senoh M, Iwasa N and Nagahama S 1995 *Jpn. J. Appl. Phys.* **34** L797

[2] Khan M A, Shatalov M, Maruska H P, Wang H M and Kuokstis E 2005 *Jpn. J. Appl. Phys.* **44** 7191

[3] Zhang M and Ban S L 2009 *Chin. Phys.* B **18** 4449

[4] Gil B 1998 *Group Nitride Semiconductor Compounds* (Oxford: Clarendon)

[5] Kim M H, Schubert M F, Dai Q, Kim J K, Schubert E F, Piprek J and Park Y 2007 *Appl. Phys. Lett.* **91** 183507

[6] Kuo Y K, Chang J Y, Tsai M C and Yen S H 2009 *Appl. Phys. Lett.* **95** 011116

[7] Takeuchi T, Amano A and Akasaki I 2000 *Jpn. J. Appl. Phys.* **39** 413

[8] Sizov D S, Bhat R, Napierala J, Gallinat C, Song K and Zah C 2009 *Appl. Phys. Express* **2** 071001

[9] Masui H, Schmidt M, Fellows N, Yamada H, Iso K, Speck J S, Nakamura S and DenBaars S P 2009 *Phys. Status Solidi* A **206** 203

[10] Schmidt M C, Kim K C, Sato H, Fwllows N and Masui H 2007 *Jpn. J. Appl. Phys.* **46** L126

[11] Sato H, Chung R B, Hirasawa H, Fellows N, Masui H, Wu F, Saito M, Fujito K, Speck J S, DenBaars S P and Nakamura S 2008 *Appl. Phys. Lett.* **92** 221110

[12] Tyagi A, Lin Y D, Cohen D A, Saito M, Fujito K, Speck J S, DenBaars S P and Nakamura S 2008 *Appl. Phys. Express* **1** 091103

[13] Asamizu H, Saito M, Fujito K, Speck J S, DenBaars S P and Nakamura S 2009 *Appl. Phys. Express* **2** 021002

[14] Masui H, Cruz S C, Nakamura S and DenBaars S P 2009 *J. Electron. Mater.* **38** 756

[15] Park S H and Chuang S L 1999 *Phys. Rev.* B **59** 4725

[16] Yamaguchi A A 2008 *Phys. Status Solidi* C **5** 2329

[17] Yamaguchi A A 2007 *Jpn. J. Appl. Phys.* **46** L789

[18] Fellows N, Sato H, Masui H, DenBaars S P and Nakamura S 2008 *Jpn. J. Appl. Phys.* **47** 7854

[19] Park S H and Ahnb D 2007 *Appl. Phys. Lett.* **90** 013505

[20] Ueda M, Funato M, Kojima K, Kawakami Y, Narukawa Y and Mukai T 2008 *Phys. Rev.* B **78** 233303

[21] Masui H, Asamizu1 H, Tyagi A, DeMille N F, Nakamura S and DenBaars S P 2009 *Appl. Phys. Express* **2** 071002

[22] Alemu A, Gil B, Julier M and Nakamura S 1998 *Phys. Rev.* B **57** 3761

[23] Hao G H and Chen Y H 2008 *Chin. Phys. Lett.* **25** 4139

[24] Ghosh S, Waltereit P, Brandt O, Grahn H T and Ploog K H 2002 *Phys. Rev.* B **65** 075202

[25] Ghosh S, Misra P, Grahn H T, Imer B, Nakamura S, DenBaars S P and Speck J S 2005 *J. Appl. Phys.* **98** 026105

[26] Ghosh S, Misra P, Grahn H T, Imer B, Nakamura S, DenBaars S P and Speck J S 2006 *Phys. Status Solidi* B **243** 1441

[27] Hao G D, Chen Y H and Hao Y F 2009 *Jpn. J. Appl. Phys.* **48** 041001

[28] Chuang S L and Chang C S 1996 *Phys. Rev.* B **54** 2491

[29] Kumagai M, Chuang S L and Ando H 1998 *Phys. Rev.* B **57** 15303

[30] Chuang S L 1995 *Physics of Optoelectronic Devices* (New York: Wiley) Chap. 4